Dosimetric Analysis of ^{177}Lu-cG250 Radioimmunotherapy in Renal Cell Carcinoma Patients: Correlation with Myelotoxicity and Pretherapeutic Absorbed Dose Predictions Based on ^{111}In-cG250 Imaging

Alexander B. Stillebroer*[1,2], Catharina M.L. Zegers*[2], Otto C. Boerman[2], Egbert Oosterwijk[1], Peter F.A. Mulders[1], Joseph A. O'Donoghue[3], Eric P. Visser[2], and Wim J.G. Oyen[2]

[1]*Department of Urology, Radboud University Nijmegen Medical Centre, Nijmegen, The Netherlands;* [2]*Department of Nuclear Medicine, Radboud University Nijmegen Medical Centre, Nijmegen, The Netherlands; and* [3]*Department of Medical Physics, Memorial Sloan-Kettering Cancer Center, New York, New York*

This study aimed to estimate the radiation absorbed doses to normal tissues and tumor lesions during radioimmunotherapy with ^{177}Lu-cG250. Serial planar scintigrams after injection of ^{111}In-cG250 or ^{177}Lu-cG250 in patients with metastasized renal cell carcinoma were analyzed quantitatively. The estimated radiation doses were correlated with observed hematologic toxicity. In addition, the accuracy of the predicted therapeutic absorbed doses, based on diagnostic ^{111}In-cG250 data, were determined. **Methods:** Twenty patients received a diagnostic tracer activity of ^{111}In-cG250 (185 MBq), followed by radioimmunotherapy with ^{177}Lu-cG250. The administered activity of ^{177}Lu-cG250 was escalated by entering 3 patients at each activity level starting at 1,110 MBq/m^2, with increments of 370 MBq/m^2. After each diagnostic and therapeutic administration, whole-body scintigraphic images and pharmacokinetic data were acquired. Hematologic toxicity was graded using the Common Toxicity Criteria, version 3.0. Diagnostic ^{111}In-cG250 data were used to simulate ^{177}Lu and ^{90}Y data by correcting for the difference in physical decay. Absorbed doses were calculated for the whole body, red marrow, organs, and tumor metastases for the therapeutic ^{177}Lu-cG250, simulated ^{177}Lu-cG250, and simulated ^{90}Y-cG250 data. **Results:** Observed hematologic toxicity, especially platelet toxicity, correlated significantly with the administered activity ($r = 0.85$), whole-body absorbed dose ($r = 0.65$), and red marrow dose ($r = 0.62$ and 0.75). An inverse relationship between the mass and absorbed dose of the tumor lesions was observed. Calculated mean absorbed doses were similar for the simulated and measured ^{177}Lu-cG250 data. Absorbed doses (whole body and red marrow) based on the simulated ^{177}Lu-cG250 data correlated with the observed platelet toxicity ($r = 0.65$ and 0.82). The tumor–to–red marrow dose ratio was higher for radioimmunotherapy with ^{177}Lu-cG250 than for radioimmunotherapy with ^{90}Y-cG250, indicating that ^{177}Lu has a wider therapeutic window for radioimmunotherapy with cG250 than ^{90}Y. **Conclusion:** In patients with metastasized renal cell carcinoma, hematologic toxicity after treatment with ^{177}Lu-cG250 can be predicted on the basis of administered activity and whole-body and red marrow–absorbed dose. Diagnostic ^{111}In-cG250 data can be used to accurately predict absorbed doses and myelotoxicity of radioimmunotherapy with ^{177}Lu-cG250. These estimations indicate that in these patients, higher radiation doses can be guided to the tumors with ^{177}Lu-cG250 than with ^{90}Y-cG250.

Key Words: radioimmunotherapy; cG250; predictive dosimetry; myelotoxicity

J Nucl Med 2012; 53:82–89
DOI: 10.2967/jnumed.111.094896

Renal cell carcinoma (RCC) is a disease with approximately 58,000 new patients each year in the United States and accounts for 3% of all malignancies (*1*). The only curative option to date for RCC is (partial) nephrectomy. Prognosis of untreated metastasized RCC is poor, with a median survival of 12 mo. With the advent of targeted agents, this prognosis has increased dramatically, more than doubling overall survival (*2*). However, side effects of these compounds are common and often severe (*3*). Therefore, we aim to develop an effective radioimmunotherapeutic approach for the treatment of RCC using the radiolabeled anti-CAIX antibody cG250.

The main goal in radioimmunotherapy is to maximize the absorbed dose to the tumor, while maintaining the dose to healthy tissues at acceptable levels. The dose-limiting normal tissue in radioimmunotherapy is the red marrow. Thrombocytopenia and leukopenia are generally the initial and most severe manifestations of myelotoxicity after radioimmunotherapy (*4*).

In several studies, methods are defined to estimate the red marrow dose based on blood activity data or planar scintigrams (*5–8*). Previous studies on the relationship between radiation dose estimates and myelotoxicity were variable (*7,9–15*). Results might have been influenced by the

Received Jun. 24, 2011; revision accepted Sep. 7, 2011.
For correspondence or reprints contact: Otto C. Boerman, Radboud University Nijmegen Medical Centre, Department of Nuclear Medicine, P.O. Box 9101, 6500 HB Nijmegen, The Netherlands.
E-mail: o.boerman@nucmed.umcn.nl
*Contributed equally to this work.
Published online Dec. 12, 2011.

used method to calculate the red marrow dose, the radionuclide used, or patient-specific factors. Recently, Baechler et al. showed, for example, that the elapsed time since the last chemotherapy is an important parameter in the prediction of toxicity (*16*).

The ability to predict the therapeutic dose to tumor lesions and healthy organs could provide tools for treatment planning. For individual dosing, each radioimmunotherapy treatment can be preceded by a diagnostic infusion of the same monoclonal antibody (mAb) labeled with a γ-emitter (*11*). The analysis of the images of an antibody labeled with ^{111}In could potentially be used to predict the targeting of the same antibody labeled with the β-emitting radionuclide ^{90}Y or ^{177}Lu. In a study of DeNardo et al., mAb Lym-1 labeled with ^{111}In was used to calculate the absorbed doses for ^{90}Y-Lym-1 in patients with non-Hodgkin lymphoma (*17*). Vallabhajosula et al. used ^{111}In-J591 as a surrogate for ^{90}Y-J591 (*10*). However, because ^{90}Y is not suitable for imaging as it is a pure β-emitting radionuclide, the accuracy of these dosimetric predictions could not be proven.

During a phase I study at our institution, patients with progressive clear cell RCC could receive multiple therapeutic doses of ^{177}Lu-cG250. Before each therapeutic administration, patients received a diagnostic infusion with ^{111}In-cG250. We used the pharmacokinetic and scintigraphic data to estimate radiation doses of the therapeutic injections to normal tissues and metastases and investigated whether these doses correlated with the observed hematologic toxicity. We investigated whether the dosimetric analysis of the diagnostic injections could be used to predict the radiation doses of the therapeutic injections after the first treatment cycle. Furthermore, absorbed dose predictions were made for radioimmunotherapy with ^{90}Y-cG250 to determine the most suitable β-emitter for radioimmunotherapy with the radiolabeled anti-CAIX antibody in these patients.

MATERIALS AND METHODS

Patients

Dosimetric data of 20 patients with progressive metastasized RCC (16 men, 4 women) who had all undergone a nephrectomy of the tumorous kidney were included. The mean age of the patients was 58 y (range, 29–74 y). The study (Clinical Trials NCT00142415) was approved by the regional Medical Ethical Review Committee of the Radboud University Nijmegen Medical Centre and the Institutional Review Board of the Ludwig Institute for Cancer Research. The study was monitored by Omnicare Corp., commissioned by the Ludwig Institute for Cancer Research. Written informed consent was obtained from all patients before study entry.

mAb cG250 and Radiolabeling

cG250 is a high-affinity ($Ka = 4 \times 10^9\ M^{-1}$) chimeric, IgG1 mAb, reactive with the CAIX antigen, a transmembrane glycoprotein overexpressed on the cell surface of most (>95%) clear cell RCCs (*18*). Vials (10 mg/mL) of clinical-grade cG250 were obtained from the Ludwig Institute for Cancer Research. cG250 was conjugated with DOTA (Macrocyclics) as described previously (*19*) at Memorial Sloan-Kettering Cancer Center. The cG250–DOTA conjugate was radiolabeled with ^{111}In (Covidien) for tracer injections in a 0.25 M ammonium acetate buffer, pH 5.4, for 30 min at 45°C. cG250–DOTA was labeled with ^{177}Lu (IDB Holland) for therapeutic injections in a 0.25 M ammoniumacetate buffer, pH 5.4, for 60 min at 45°C. All labeling procedures using ^{111}In or ^{177}Lu were performed under strict metal-free conditions. All radiolabeled cG250 preparations were purified by gel filtration on a PD-10 column (GE Healthcare) eluted with phosphate-buffered saline supplemented with 5 mM diethylenetriaminepentaacetic acid and 10 mM ascorbic acid. For all preparations, the amount of non–mAb-associated radiolabel was determined by instant thin-layer chromatography (ITLC) with ITLC silica gel strips (Pall Corp. Life Sciences), using 0.1 M citrate buffer, pH 6.0, as the mobile phase (R_f, 0 for radiolabeled antibody and 0.8–1 for free and chelated radionuclides) (*18*). The radiochemical purity was greater than 99% for ^{111}In-DOTA-cG250 and 99.3% ± 0.9% for ^{177}Lu-DOTA-cG250. The immunoreactive fraction determined as described previously was 90.1% ± 5.3% and 89.8% ± 6.8% for the ^{111}In-cG250 and ^{177}Lu-cG250 preparations, respectively.

Study Design

In this phase I study, the maximum-tolerated dose (MTD) of ^{177}Lu-cG250 radioimmunotherapy was determined by entering 3 patients at each activity level, starting at 1,110 MBq/m^2, with dose increments of 370 MBq/m^2. The MTD was defined as the administered activity at which no more than 1 of 6 patients showed dose-limiting toxicity (DLT). DLT was defined as grade 3 or greater nonhematologic toxicity or grade 4 or greater hematologic toxicity (platelets $< 25 \times 10^9$/L or leukocytes $< 1.0 \times 10^9$/L), lasting for more than 4 wk, or the occurrence of hemoglobin less than 4.9 mmol/L or thrombocytes less than 10×10^9/L at any time point. The administered ^{177}Lu dose was calculated with the formula from a study of Mosteller (*20*).

Toxicity was monitored weekly, by determining the hematologic and blood chemistry laboratory parameters, and was scored according to the U.S. National Cancer Institute Common Toxicity Criteria (version 3.0).

All radioimmunotherapy administrations were preceded by a diagnostic tracer of ^{111}In-cG250 (185 MBq; 10 mg of cG250; total volume, 5 mL) to visually assess preferential uptake of the radiolabeled antibody in the tumor lesions and to exclude the presence of human antichimeric antibodies.

Patients received 1 ($n = 23$), 2 ($n = 13$), or 3 ($n = 4$) cycles of treatment. The clinical results of this study will be described in another paper. In the current paper, dosimetric analysis of the first treatment cycle of the first 20 patients is performed. Analysis of the last 4 patients has not been performed because of logistic reasons. Dosimetric analyses of the second and third treatment cycles were not incorporated, to avoid confusion and because of the limited amount of data.

Imaging and Pharmacokinetics

After each ^{111}In-cG250 administration, 3 whole-body scintigrams were acquired (directly after injection, at 2–4 d after injection, and at 5–7 d after injection). The images were recorded in conjugate view using a double-head γ-camera (ECAM, Siemens Inc.), equipped with parallel-hole medium-energy collimators. Symmetric energy windows were set at 15% of the ^{111}In photopeaks at 172 and 247 keV. Images consisted of summed counts collected in both windows. The scan speed was 8, 6, and 4 cm/min

at days 0, 2–4, and 5–7 after injection, respectively. The matrix size was 256 × 1,024, with a pixel size of 2.4 × 2.4 mm. Images obtained after infusion of ^{177}Lu-cG250 were recorded using a symmetric 15% energy window of 208 keV at the same time points and with the same scan speeds as after the ^{111}In-cG250 infusion.

Blood samples were drawn directly; at 30, 60, and 120 min; and at 2–4 and 5–7 d after the ^{111}In-cG250 and ^{177}Lu-cG250 infusions. The activity concentration in the serum from these samples was counted in a shielded 7.6-cm (3-in) well-type γ-counter (Wizard; LKB/Wallac, Perkin-Elmer). To correct for radioactive decay, reference samples containing a known fraction of the administered activity were measured simultaneously. The activity concentrations in the serum samples were corrected for the hematocrit content in the patient's blood to obtain blood activity concentrations.

Dosimetry

The radiation absorbed doses to the whole body, liver, red marrow, lungs, heart, testes, normal kidney, and metastases delivered by therapeutic ^{177}Lu-cG250 injections were calculated according to the MIRD scheme (*21*).

Metastatic lesions measurable on CT and visualized in at least 1 of the scintigraphic images were analyzed. The volume ($V = \frac{1}{6}\pi \times$ length × width × height) and background-correction factor of the metastatic lesions were derived from CT. Tumor volumes were converted to mass, assuming that the tumor density equals 1 g/cm^3.

Residence times of the source organs and metastases were calculated using SPRIND, a software package for integrated data processing for internal dose assessment (*6*). Regions of interest for source organs and tumors were drawn on both anterior and posterior scintigraphic images. The counts within the regions of interest were corrected for attenuation and background contribution as described by Visser et al. (*6*). The geometric mean was calculated, and the data were integrated over time using the trapezoid method. After the last scan, SPRIND assumes only physical decay of the radionuclide in the source organs. To calculate the absorbed doses, residence times were imported into the software package OLINDA/EXM (*22*). Radiation absorbed doses to the whole body and organs of interest were calculated using the adult male and the adult female phantom. The sphere model was used to determine the radiation absorbed doses to the metastases (*22*).

The red marrow–absorbed dose was calculated using 2 methods. First, the absorbed dose to the red marrow was calculated using the scintigraphic images. In SPRIND, regions of interest were drawn over the left and right part of the cranium. The residence times of the left and right cranium were summed and divided by the fraction of the red marrow mass in the cranium to the total red marrow mass in the body, for which the default value of 0.119 was taken from the reference man according to the International Commission on Radiological Protection (*23*). The second method was the blood-based method as described by Shen et al. (*5*). This method was also implemented in SPRIND (Visser et al. (*6*)).

Predictive Dosimetry

Dosimetric data obtained after the diagnostic ^{111}In-cG250 infusion were used to calculate the predicted therapeutic doses from ^{177}Lu-cG250, assuming identical biodistribution and biologic clearance of ^{111}In-cG250 and ^{177}Lu-cG250. Simulated ^{177}Lu scans were generated by correcting the ^{111}In whole-body scintigrams for the difference in physical decay of ^{111}In and ^{177}Lu. Each ^{111}In-cG250 scintigram (anterior and posterior images) was multiplied pixelwise by $e^{t(\lambda_{In} - \lambda_{Lu})}$ (t = time after injection) to obtain simulated whole-body scintigrams for ^{177}Lu. The resulting simulated ^{177}Lu scintigrams were used to calculate residence times with SPRIND and the simulated absorbed doses with OLINDA for the organs of interest and metastases.

The blood-based red marrow–absorbed dose for ^{177}Lu was also simulated. To simulate the blood residence time of ^{177}Lu, ^{111}In-cG250 blood data and reference samples were used to determine the biologic clearance of activity from the blood, and physical clearance was incorporated by multiplication with $e^{-\lambda_{Lu}t}$.

To provide insight in the absorbed doses for radioimmunotherapy with ^{90}Y-cG250, the same methods were used to simulate ^{90}Y data.

Statistical Analysis

The Pearson correlation coefficient was determined to evaluate the relationship between the image- and the blood-based methods to calculate the red marrow dose, between tumor mass and tumor-absorbed dose, and between calculated absorbed doses for ^{177}Lu-cG250 and simulated data. Hematologic toxicity was correlated with administered activity, whole-body dose, red marrow dose, and the electron contribution of the red marrow dose. In addition, the relationship between hematologic toxicity and the simulated whole-body and red marrow dose was determined. The tumor–to–red marrow dose ratios were determined to compare (simulated) ^{177}Lu-cG250 data with simulated ^{90}Y-cG250 data.

RESULTS

Patients

All 20 patients completed the full course of ^{111}In-cG250 and ^{177}Lu-cG250 radioimmunotherapy. In each patient, only data from the first treatment cycle were used for dosimetric analysis. DLT was noted in 1 patient at the 1,850 MBq/m^2 activity level. Because the other 5 patients who received this activity showed no DLT, the administered activity was further incremented. At the 2,590 MBq/m^2 activity level, DLT was seen in all 3 patients; therefore, the administered activity was reduced to 2,405 MBq/m^2. This activity level proved to be safe in 6 patients (only 1 of 6 patients had DLT), and by definition the latter dose was designated as the MTD.

Data

Imaging data after the treatment were used to determine the absorbed dose in the organs of interest and metastases after administration with ^{177}Lu-cG250. The diagnostic ^{111}In-cG250 data were also used to evaluate the predictive value of the simulated ^{177}Lu-cG250 data and to calculate absorbed doses for radioimmunotherapy with ^{90}Y-cG250.

The ^{177}Lu-cG250 data of 2 patients had to be excluded from the analysis because of incomplete or inconsistent scintigraphic data. Another patient (patient 17) showed an unexpected high uptake in the liver and red marrow after injection of ^{177}Lu-cG250 because of the presence of human antichimeric antibodies or the presence of aggregates in the radiolabeled antibody preparation. The dosimetric results of this patient were therefore excluded from the analysis. Subsequently, dosimetry data of 17 patients have been analyzed in this study.

For the ^{177}Lu-cG250 and ^{111}In-cG250 data, 40 and 48, respectively, metastases were used for tumor-absorbed dose calculations. The weight of these tumors, determined on the CT images, ranged from 0.6 to 319 g.

A complete set of blood activity data was acquired from 15 (^{177}Lu-cG250) and 16 (^{111}In-cG250) patients. These pharmacokinetic data were used to calculate the blood-based red marrow–absorbed dose in these patients.

^{177}Lu-cG250 Radiation Doses

The estimated mean radiation absorbed doses after ^{177}Lu-cG250 radioimmunotherapy were 0.24 ± 0.04 mGy/MBq for the whole body, 0.49 to 1.90 mGy/MBq for the healthy organs, and 0.44 ± 0.07 mGy/MBq (image-based) and 0.35 ± 0.07 mGy/MBq (blood-based) for the red marrow (Table 1).

The results of the image- and blood-based methods to calculate the red marrow–absorbed dose correlated significantly ($r = 0.68$, $P = 0.005$, Fig. 1). Observed thrombocyte toxicity correlated significantly with the administered activity ($r = 0.85$), whole-body dose ($r = 0.65$), and image- and blood-derived red marrow dose ($r = 0.62$ and 0.75, respectively, Fig. 2). Leukocyte toxicity correlated significantly with the administered activity ($r = 0.66$) and the blood-based red marrow dose ($r = 0.53$). However, there was no significant relationship between the leukocyte toxicity and the whole-body dose or the image-based red marrow dose. The correlations are summarized in Tables 2 and 3.

Absorbed doses to the tumor lesions varied widely from 0.47 to 17.29 mGy/MBq. The mean tumor–to–red marrow dose ratio for ^{177}Lu-cG250 was 13.0 and 16.3, respectively, for the image- and blood-based methods. The total tumor dose during the first treatment cycle varied from 1.9 to 92.0 Gy. The radiation dose to the tumor lesions correlated inversely with the mass of the tumor lesions ($r = -0.44$, $P < 0.005$, Fig. 3).

Simulated ^{177}Lu-cG250 Radiation Doses

The simulated ^{177}Lu-cG250 absorbed doses for the whole body, organs, and metastases based on the diagnostic ^{111}In-cG250 data are presented in Table 1. The calculated doses were similar to the doses as derived from the ^{177}Lu-cG250 images (Fig. 4). However, for the individual patient, slight differences were found. For example, the largest differences in calculated red marrow dose were −20.0% and 14.9% for the image-based method and −25.5% and 7.7% for the blood-based method. There is a significant correlation between the ^{177}Lu-cG250 and simulated absorbed dose calculations for the whole body, liver, heart wall, red marrow, lungs, testes, and metastases ($r = 0.82$–0.98, $P < 0.001$). In contrast, the calculated kidney-absorbed dose of the simulated data in comparison to the ^{177}Lu-cG250 data did not show any correlation ($r = -0.28$).

Thrombocyte and leukocyte toxicity correlated significantly with the simulated whole-body and red marrow (image-based) dose ($r = 0.55$–0.82, $P < 0.05$). In addition, thrombocyte toxicity correlated significantly with the blood-based red marrow dose ($r = 0.65$, $P < 0.01$). These correlations are summarized in Tables 2 and 3. For the simulated ^{177}Lu-cG250 data, the tumor–to–red marrow dose ratio was 11.9 (image-based) and 15.7 (blood-based).

Simulated ^{90}Y-cG250 Radiation Doses

Simulated mean radiation absorbed doses for radioimmunotherapy with ^{90}Y-cG250 were 0.64 mGy/MBq for the whole body, 1.45–4.32 mGy/MBq for the normal organs, and 0.90 mGy/MBq (image-based) and 0.81 mGy/MBq (blood-based) for the red marrow (Table 1). Radioimmunotherapy with ^{90}Y-cG250 resulted in a theoretic mean absorbed dose of 9.76 mGy/MBq to the metastases. The tumor–to–red marrow dose ratio for this simulated ^{90}Y-cG250 data was 10.8 and 12.0 for, respectively, the image- and blood-based methods. Mean absorbed doses to the bone marrow (mGy/MBq) were approximately 2–3 times higher than the (simulated) ^{177}Lu-cG250 data (Fig. 4).

TABLE 1
Radiation Absorbed Dose in Whole Body, Organs, and Metastases for ^{177}Lu-cG250, Simulated ^{177}Lu-cG250, and Simulated ^{90}Y-cG250 (mGy/MBq)

	^{177}Lu-cG250 radioimmunotherapy			Simulated ^{177}Lu-cG250 radioimmunotherapy			Simulated ^{90}Y-cG250 radioimmunotherapy		
Organs	Mean ± SD	Minimum	Maximum	Mean ± SD	Minimum	Maximum	Mean ± SD	Minimum	Maximum
Whole body	0.24 ± 0.04	0.19	0.36	0.25 ± 0.03	0.21	0.33	0.64 ± 0.08	0.57	0.82
Liver	1.26 ± 0.25	0.93	1.75	1.22 ± 0.23	0.93	1.75	3.03 ± 0.63	2.27	4.49
Heart wall	0.76 ± 0.16	0.47	1.12	0.68 ± 0.13	0.47	0.93	2.05 ± 0.38	1.41	2.69
Red marrow									
Image-based	0.44 ± 0.07	0.32	0.62	0.41 ± 0.06	0.35	0.57	0.90 ± 0.11	0.78	1.11
Blood-based	0.35 ± 0.07	0.24	0.46	0.31 ± 0.07	0.21	0.46	0.81 ± 0.21	0.47	1.23
Kidney	1.30 ± 0.35	0.78	1.92	1.43 ± 0.49	0.76	2.57	3.77 ± 1.26	2.00	6.24
Lungs	0.49 ± 0.13	0.34	0.74	0.48 ± 0.10	0.37	0.65	1.45 ± 0.35	1.06	2.08
Testes	1.90 ± 0.45	1.20	2.70	1.64 ± 0.36	1.11	2.36	4.32 ± 0.99	2.84	6.26
Metastases	5.72 ± 4.52	0.47	17.29	4.86 ± 4.69	0.52	19.92	9.76 ± 8.88	1.31	37.52

Data are mean ± SD.

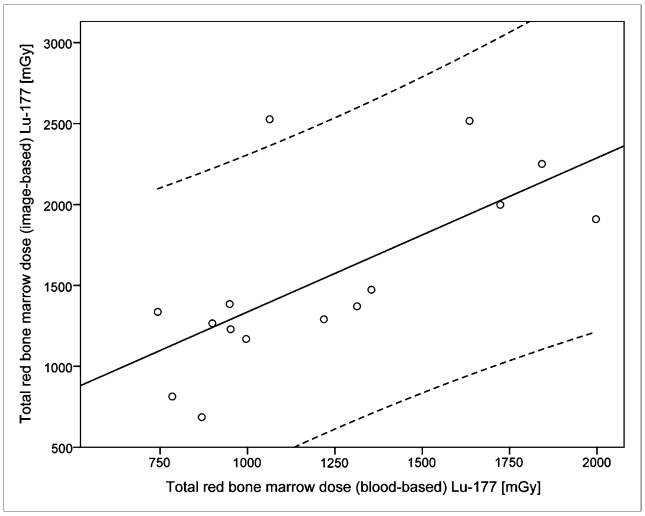

FIGURE 1. Total red marrow dose based on image-based method plotted against total red marrow dose based on blood-based method ($r = 0.68$, $P = 0.005$). Striped line is 95% confidence interval.

DISCUSSION

This study was designed to estimate the radiation absorbed doses to normal tissues and tumor lesions during radioimmunotherapy with ^{177}Lu-cG250 in patients with clear cell RCC. Radiation-induced myelotoxicity was dose limiting in these patients. An accurate estimation of the red marrow dose is essential for reliable predictions of the maximum activity that can be administered safely. The radiation dose to the red marrow can be estimated using the activity levels in the blood (*5*), as long as the radiolabeled antibody does not bind specifically to the cells in the bone marrow. However, various other imaging methods to estimate the red marrow dose have been described (*6–8*). DeNardo et al. showed, for example, that an image-based method, unlike the blood-based method, was able to predict thrombocytopenia and leukopenia (*7*). In the present study, both the blood-based method and an image-based method were used to estimate the red marrow dose. The calculated mean absorbed doses for both methods were in the same range, 0.35 versus 0.44 mGy/MBq. In addition, there was a significant correlation between the red marrow dose calculated with both methods ($r = 0.68$, $P = 0.005$). The blood-based red marrow–absorbed dose was 0.35 ± 0.07 mGy/MBq for ^{177}Lu-cG250, which is somewhat higher than reported by Vallabhajosula et al. (*10*) for radioimmunotherapy with ^{177}Lu-J591 (0.32 ± 0.10 mGy/MBq). This slight difference in red marrow dose is in agreement with the difference in MTD: 2,405 MBq/m^2 for ^{177}Lu-cG250 and 2,590 MBq/m^2 for ^{177}Lu-J591 (*10*).

In this patient population, the observed hematologic toxicity ranged from grade 0 to grade 4. The relationship among hematologic toxicity, the administered activity, and the absorbed dose calculations (whole body, red marrow) were analyzed. Myelotoxicity, especially thrombocyte toxicity, correlated significantly with the administered activity, whole-body dose, and red marrow dose. The correlation between myelotoxicity and the blood-based red marrow dose was higher than that between myelotoxicity and the image-based method. Therefore, in these patients, the blood-based method was a better predictor of myelotoxicity. Although the overall correlation between calculated red marrow dose and observed myelotoxicity is high, individual patients have had more severe toxicity than others at the same dose level, limiting the use of calculated dosimetry as a predictor of the biologic event of myelotoxicity. Larger patient cohorts will have to be studied to accurately determine whether dosimetric analyses can be used to predict the toxicity of individual patients.

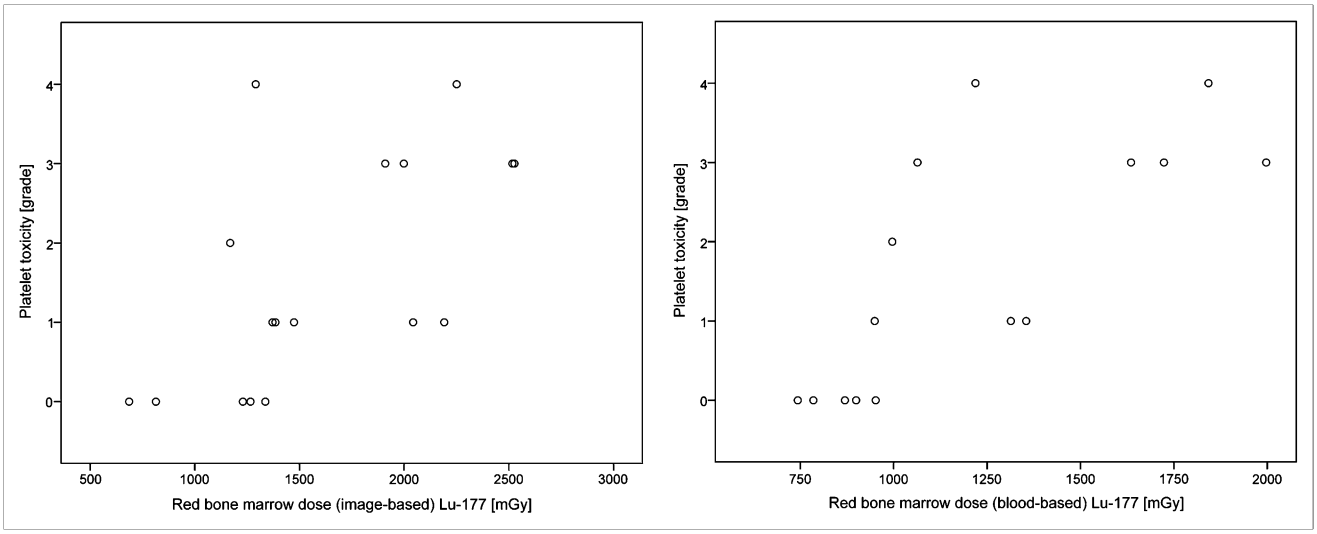

FIGURE 2. Platelet toxicity (grade according to Common Toxicity Criteria, version 3.0) plotted against red marrow dose based on image-based method ($r = 0.62$, $P = 0.007$) and blood-based method ($r = 0.75$, $P = 0.001$).

TABLE 2
Pearson Correlation Coefficients (and Its 2-Tailed Significance) Between Toxicity Grade and Administered Activity or Absorbed Dose Calculations for ^{177}Lu-cG250

Toxicity	Administered activity (MBq)	Total whole-body dose	Total red marrow dose (image-based)	Total red marrow dose (blood-based)
Thrombocyte				
Pearson correlation	0.85*	0.65*	0.62*	0.75*
Significance (2-tailed)	<0.001	0.005	0.007	0.001
Leukocyte				
Pearson correlation	0.66*	0.32	0.27	0.53†
Significance (2-tailed)	0.001	0.214	0.287	0.043
N	20	17	17	15

*Correlation is significant at 0.01 level.
†Correlation is significant at 0.05 level.

In a series of previous radioimmunotherapy studies, no correlations were found between radiation absorbed doses and myelotoxicity (*7,9,12,13*). On the other hand, Divgi et al. (*14*) showed a significant correlation between the whole-body absorbed dose and the hematologic toxicity after radioimmunotherapy with ^{131}I-cG250. Juweid et al. (*15*) described a significant correlation between the calculated red marrow dose and hematologic toxicity for radioimmunotherapy with a ^{131}I-labeled anti–carcinoembryonic antigen antibody. Furthermore, Vallabhajosula et al. (*10*) showed that myelotoxicity correlated with the administered activity and red marrow–absorbed dose for radioimmunotherapy with ^{177}Lu-J591. Moreover, Vallabhajosula et al. (*10*) showed that the blood-based red marrow dose correlated best with the fractional decrease of thrombocytes. Similarly, in our study the blood-based red marrow dose correlated best with the thrombocyte toxicity grade ($r = 0.75$).

Normal organs receiving the highest absorbed doses were the liver, kidney, and testes, with a mean dose of 1.26, 1.30, and 1.90 mGy/MBq, respectively. This dose was 5.8, 6.0, and 8.8 Gy, respectively, at MTD, for a mean body surface area of 1.79 m (*2,24*). The liver and kidney doses were well below the threshold for deterministic effects, which are, respectively, 30 and 23 Gy (*25,26*). On the basis of experiments using external-beam radiation therapy, it was suggested that a fractionated dose of 2 Gy or more to the testes could cause permanent infertility (*27*). This dose was exceeded for radioimmunotherapy with ^{177}Lu-cG250, but the fertility status of men in this study was not investigated. However, in dosimetry, the testis dose is primarily derived from the blood-pool activity in and around the organ and not from the organ itself, possibly leading to an overestimation of the testis dose.

To accurately estimate the tumor-absorbed dose, the tumor-specific volume and background-correction factor were determined by CT. The total tumor dose varied widely from 0.47 to 17.3 mGy/MBq, mainly because of differences in uptake of the radiolabeled antibody in the lesions. In 17 of the 40 tumors, ^{177}Lu-cG250 activity was highest at the last scintigraphic acquisition, indicating that there is a slow accumulation of radiolabeled cG250 during 5–7 d. Because there were no scintigraphic data available beyond 5–7 d after injection, the tumor-absorbed dose might be slightly underestimated if only physical decay is considered. Conversely, an overestimation of the tumor dose could have occurred because of biologic clearance of the radiolabel

TABLE 3
Pearson Correlation Coefficients (and Its 2-Tailed Significance) Between Toxicity Grade and Administered Activity or Absorbed Dose Calculations for Simulated ^{177}Lu-cG250 (mGy)

Toxicity	Total whole-body dose	Total red marrow dose (image-based)	Total red marrow dose (blood-based)
Thrombocyte			
Pearson correlation	0.82*	0.81*	0.65*
Significance (2-tailed)	<0.001	<0.001	0.007
Leukocyte			
Pearson Correlation	0.61*	0.55†	0.49
Significance (2-tailed)	0.006	0.015	0.054

*Correlation is significant at 0.01 level.
†Correlation is significant at 0.05 level.

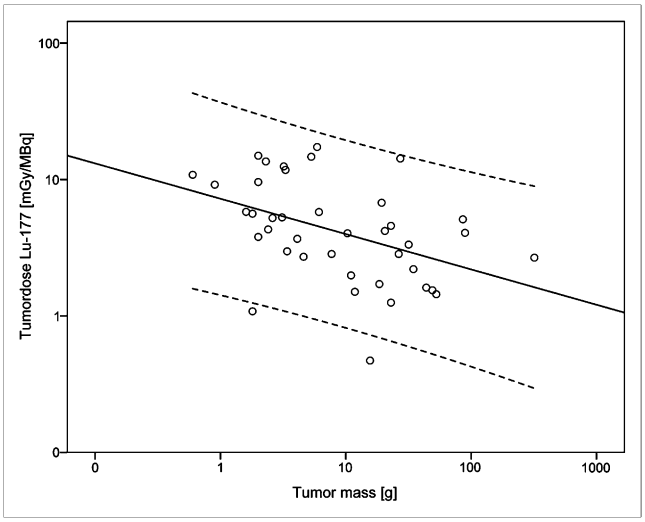

FIGURE 3. Absorbed dose in metastases for ^{177}Lu-cG250 radioimmunotherapy plotted against weight of metastatic lesions on logarithmic scales ($r = -0.44$, $P < 0.005$). Striped line is 95% confidence interval.

after the last imaging time point. As described in several other studies (*9,11,28*), an inverse relationship between tumor dose and tumor mass was observed in this study. Tumor doses exceeding 50 Gy are considered to be required to achieve a therapeutic response in these patients (*29*). In this study, only 2 of 40 tumor lesions received a tumor dose of greater than 50 Gy during the first treatment cycle. Twelve of 40 tumors received a tumor dose greater than 25 Gy during the first cycle, suggesting that for these tumors a tumor-sterilizing dose can be reached during subsequent treatment cycles.

Diagnostic ^{111}In-cG250 data were used to predict therapeutic absorbed doses by correcting scintigrams and blood activity data for the physical decay difference between the radionuclides. The simulated absorbed doses were compared with the measured absorbed doses for ^{177}Lu-cG250. There was no significant difference between the mean absorbed doses for the simulated and measured ^{177}Lu-cG250 data. In addition, the simulated absorbed dose correlated significantly with the absorbed dose after radioimmunotherapy for the whole body, liver, heart wall, red marrow, lungs, testes, and tumor lesions ($r = 0.818$–0.982, $P < 0.001$). The calculated kidney-absorbed dose for ^{177}Lu-cG250 in comparison to the simulated data based on the ^{111}In-cG250 data did not correlate, because of the high and time-dependent activity in the colon, overlapping the kidney region. In this study, it was shown that simulations, based on diagnostic data, can be used not only to predict the absorbed doses but also to predict myelotoxicity, because the simulated whole-body and red marrow–absorbed dose correlated significantly with thrombocyte and leukocyte toxicity. These results provide tools for treatment planning, because a toxicity risk assessment can be made before radioimmunotherapy.

Another suitable radionuclide for radioimmunotherapy with cG250 is ^{90}Y (*30*). An advantage of ^{90}Y is the long range of the β-emissions, which could overcome the intratumoral heterogeneity of the antibody uptake. A disadvantage is the inability to reliably image the ^{90}Y activity distribution, because of the absence of γ-emissions. We showed that the ^{111}In-cG250 scintigrams and pharmacokinetic data could be used to accurately estimate the radiation doses after radioimmunotherapy with ^{177}Lu-cG250. Therefore, it was assumed that ^{90}Y-cG250 absorbed doses can also be predicted using the ^{111}In-cG250 data. The calculated absorbed doses (mGy/MBq) for ^{90}Y-cG250 were approximately 2–3 times higher than for ^{177}Lu-cG250—in the same range as described by Vallabhajosula et al. (*10*), who reported a 3-times higher bone marrow dose for radioimmunotherapy with ^{90}Y-J591 than with ^{177}Lu-J591. Considering the ratio of blood-based red marrow dose between ^{177}Lu and simulated ^{90}Y found in the present study and assuming this is the main determinant of MTD, the anticipated MTD of ^{90}Y-cG250 radioimmunotherapy would be around 25–28 MBq/kg, which is substantially lower than that of ^{177}Lu-cG50. However, because myelotoxicity from ^{90}Y radioimmunotherapy cannot be predicted by the blood-based red marrow dose (*10*), a clinical trial is warranted to investigate the MTD and tumor doses of ^{90}Y-cG250 radioimmunotherapy in metastasized RCC patients. A more relevant parameter to compare tumor doses of ^{90}Y and ^{177}Lu-cG250 is the ratio between the tumor and red marrow

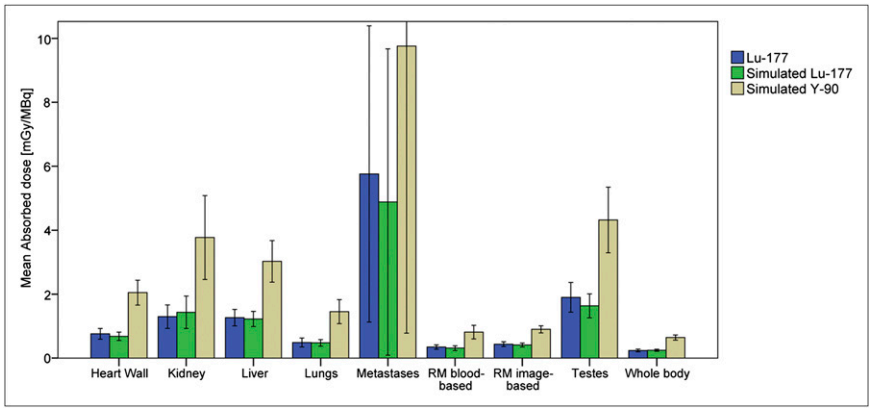

FIGURE 4. Mean absorbed dose (±SD) in organs of interest, whole body, and metastases for ^{177}Lu-cG250, simulated ^{177}Lu-, and ^{90}Y-cG250 data. RM = red marrow.

dose, rather than the absolute doses to the tumor and the red marrow. The tumor–to–red marrow dose ratio was higher for (simulated) ^{177}Lu-cG250 than for ^{90}Y-cG250. The tumor-absorbed dose depends on the accumulation of radioactive cG250. Because of the slow accumulation of cG250 in the metastases and the longer half-life of ^{177}Lu than of ^{90}Y, the radiation dose that can be guided to the tumor lesions is anticipated to be higher for radioimmunotherapy with ^{177}Lu-cG250.

CONCLUSION

In patients with RCC, hematologic toxicity, especially thrombocyte toxicity, after radioimmunotherapy with ^{177}Lu-cG250 can be predicted on the basis of administered activity and whole-body and red marrow doses. Diagnostic ^{111}In-cG250 data can be used to predict absorbed doses for radioimmunotherapy with ^{177}Lu-cG250 and ^{90}Y-cG250. In these patients, treatment with ^{177}Lu-cG250 provides a higher tumor–to–red marrow dose ratio than treatment with ^{90}Y-cG250.

DISCLOSURE STATEMENT

The costs of publication of this article were defrayed in part by the payment of page charges. Therefore, and solely to indicate this fact, this article is hereby marked "advertisement" in accordance with 18 USC section 1734.

ACKNOWLEDGMENTS

We thank all nuclear medicine technicians of the Nuclear Medicine Department of the Radboud University Nijmegen Medical Centre for the excellent acquisition, storage, and handling of the scintigrams used in this study. No other potential conflict of interest relevant to this article was reported.

REFERENCES

1. Jemal A, Siegel R, Ward E, Hao Y, Xu J, Thun MJ. Cancer statistics, 2009. *CA Cancer J Clin.* 2009;59:225–249.
2. Motzer RJ, Hutson TE, Tomczak P, et al. Sunitinib versus interferon alfa in metastatic renal-cell carcinoma. *N Engl J Med.* 2007;356:115–124.
3. Hartmann JT, Haap M, Kopp HG, Lipp HP. Tyrosine kinase inhibitors: a review on pharmacology, metabolism and side effects. *Curr Drug Metab.* 2009;10:470–481.
4. DeNardo GL, Siantar CL, DeNardo SJ. Radiation dosimetry for radionuclide therapy in a nonmyeloablative strategy. *Cancer Biother Radiopharm.* 2002;17:107–118.
5. Shen S, DeNardo GL, Sgouros G, O'Donnell RT, DeNardo SJ. Practical determination of patient-specific marrow dose using radioactivity concentration in blood and body. *J Nucl Med.* 1999;40:2102–2106.
6. Visser E, Postema E, Boerman O, Visschers J, Oyen W, Corstens F. Software package for integrated data processing for internal dose assessment in nuclear medicine (SPRIND). *Eur J Nucl Med Mol Imaging.* 2007;34:413–421.
7. DeNardo DA, DeNardo GL, O'Donnell RT, et al. Imaging for improved prediction of myelotoxicity after radioimmunotherapy. *Cancer.* 1997;80(12, suppl): 2558–2566.
8. Siegel JA, Lee RE, Pawlyk DA, Horowitz JA, Sharkey RM, Goldenberg DM. Sacral scintigraphy for bone marrow dosimetry in radioimmunotherapy. *Int J Rad Appl Instrum B.* 1989;16:553–559.
9. Behr TM, Sharkey RM, Juweid ME, et al. Phase I/II clinical radioimmunotherapy with an iodine-131-labeled anti-carcinoembryonic antigen murine monoclonal antibody IgG. *J Nucl Med.* 1997;38:858–870.
10. Vallabhajosula S, Goldsmith SJ, Hamacher KA, et al. Prediction of myelotoxicity based on bone marrow radiation-absorbed dose: radioimmunotherapy studies using ^{90}Y- and ^{177}Lu-labeled J591 antibodies specific for prostate-specific membrane antigen. *J Nucl Med.* 2005;46:850–858.
11. Brouwers AH, Buijs WC, Mulders PF, et al. Radioimmunotherapy with [^{131}I] cG250 in patients with metastasized renal cell cancer: dosimetric analysis and immunologic response. *Clin Cancer Res.* 2005;11:7178s–7186s.
12. Wiseman GA, White CA, Sparks RB, et al. Biodistribution and dosimetry results from a phase III prospectively randomized controlled trial of Zevalin radioimmunotherapy for low-grade, follicular, or transformed B-cell non-Hodgkin's lymphoma. *Crit Rev Oncol Hematol.* 2001;39:181–194.
13. Wiseman GA, White CA, Stabin M, et al. Phase I/II ^{90}Y-Zevalin (yttrium-90 ibritumomab tiuxetan, IDEC-Y2B8) radioimmunotherapy dosimetry results in relapsed or refractory non-Hodgkin's lymphoma. *Eur J Nucl Med.* 2000;27: 766–777.
14. Divgi CR, Bander NH, Scott AM, et al. Phase I/II radioimmunotherapy trial with iodine-131-labeled monoclonal antibody G250 in metastatic renal cell carcinoma. *Clin Cancer Res.* 1998;4:2729–2739.
15. Juweid ME, Zhang CH, Blumenthal RD, Hajjar G, Sharkey RM, Goldenberg DM. Prediction of hematologic toxicity after radioimmunotherapy with ^{131}I-labeled anticarcinoembryonic antigen monoclonal antibodies. *J Nucl Med.* 1999;40:1609–1616.
16. Baechler S, Hobbs RF, Jacene HA, Bochud FO, Wahl RL, Sgouros G. Predicting hematologic toxicity in patients undergoing radioimmunotherapy with ^{90}Y-ibritumomab tiuxetan or ^{131}I-tositumomab. *J Nucl Med.* 2010;51:1878–1884.
17. DeNardo GL, O'Donnell RT, Shen S, et al. Radiation dosimetry for ^{90}Y-2IT-BAD-Lym-1 extrapolated from pharmacokinetics using ^{111}In-2IT-BAD-Lym-1 in patients with non-Hodgkin's lymphoma. *J Nucl Med.* 2000;41:952–958.
18. Steffens MG, Boerman OC, Oosterwijk-Wakka JC, et al. Targeting of renal cell carcinoma with iodine-131-labeled chimeric monoclonal antibody G250. *J Clin Oncol.* 1997;15:1529–1537.
19. Lewis MR, Kao JY, Anderson AL, Shively JE, Raubitschek A. An improved method for conjugating monoclonal antibodies with N-hydroxysulfosuccinimidyl DOTA. *Bioconjug Chem.* 2001;12:320–324.
20. Mosteller RD. Simplified calculation of body-surface area. *N Engl J Med.* 1987;317:1098.
21. Loevinger R, Budinger TF, Watson EE. *MIRD Primer for Absorbed Dose Calculations*. New York, NY: The Society of Nuclear Medicine; 1988.
22. Stabin MG, Sparks RB, Crowe E. OLINDA/EXM: the second-generation personal computer software for internal dose assessment in nuclear medicine. *J Nucl Med.* 2005;46:1023–1027.
23. International Commission on Radiological Protection (ICRP). *Report of the Task Group on Reference Man*. ICRP publication 23. Ottawa, Ontario, Canada: ICRP; 1975.
24. Sacco JJ, Botten J, Macbeth F, Bagust A, Clark P. The average body surface area of adult cancer patients in the UK: a multicentre retrospective study. *PLoS ONE.* 2010;5:e8933.
25. Koral KF, Huberty JP, Frame B, et al. Hepatic absorbed radiation dosimetry during I-131 metaiodobenzylguanidine (MIBG) therapy for refractory neuroblastoma. *Eur J Nucl Med Mol Imaging.* 2008;35:2105–2112.
26. Konijnenberg M, Melis M, Valkema R, Krenning E. de JM. Radiation dose distribution in human kidneys by octreotides in peptide receptor radionuclide therapy. *J Nucl Med.* 2007;48:134–142.
27. Howell S, Shalet S. Gonadal damage from chemotherapy and radiotherapy. *Endocrinol Metab Clin North Am.* 1998;27:927–943.
28. Chatal JF, Saccavini JC, Gestin JF, et al. Biodistribution of indium-111-labeled OC 125 monoclonal antibody intraperitoneally injected into patients operated on for ovarian carcinomas. *Cancer Res.* 1989;49:3087–3094.
29. Goldenberg DM. Targeted therapy of cancer with radiolabeled antibodies. *J Nucl Med.* 2002;43:693–713.
30. Brouwers AH, Buijs WC, Oosterwijk E, et al. Targeting of metastatic renal cell carcinoma with the chimeric monoclonal antibody G250 labeled with ^{131}I or ^{111}In: an intrapatient comparison. *Clin Cancer Res.* 2003;9:3953S–3960S.